Vol. 40, No. 4 (2018) 584-593, DOI: 10.24874/ti.2018.40.04.07

Tribology in Industry

www.tribology.rs

RESEARCH

Fracture Toughness and Tribological Wear Behaviour of Micro Alloyed Pearlitic- Ferritic Ductile Cast Iron

S.O. Omole[a], A. Oyetunji[a], K.K. Alaneme[a], P.A. Olubambi[b]

[a]*Metallurgical and Materials Engineering Dept. Federal University of Technology, Akure, Nigeria,*
[b] *Centre for Nano Engineering and Tribo-corrosion, and School of Mining, Metallurgical and Chemical Engineering, University of Johannesburg, South Africa.*

Keywords:

Wear
Alloyed
Fracture
Ductile iron
Composition
Pearlitic-Ferritic

Corresponding author:

Sylvester Olanrewaju Omole, Metallurgical and Materials Engineering Dept. Federal University of Technology, Akure, Nigeria.
E-mail: sylvesteromole@yahoo.com

A B S T R A C T

Fracture toughness and wear behaviour of micro alloyed ductile iron were investigated. Hardness, fracture, fracture toughness and wear tests were carried out on the ductile irons samples (D_1, D_2, D_3, D_4 and D_5), containing micro alloyed nickel, molybdenum, copper and chromium in an amount of 0.2 % or less. They were characterized using optical metallurgical microscope and they contained pearlitic- ferritic matrix structure. They were subjected to wear test at room temperature based on pin-on-disk operation. Fracture surfaces and the wear track were studied using scanning electron microscope and found that the fracture surfaces majorly consist of fibrous with little cleavage fracture pattern in some samples. Wear mechanism is delamination with adhesive wear behavior. The specific wear rate was found to decrease with increasing hardness of the material and coefficient of friction of the ductile irons during test.

1. INTRODUCTION

Wear is a phenomenon that we encounter frequently on components in service, in which the magnitude depends on the tribological conditions such as material properties, equipment, magnitude of the abrasion and the environment [1]. According to Meng [2] wear and friction coefficient are not inherent properties of a material rather their dependence is on the variation of the grain structure and the mechanical properties presented across the interface of the material. Wear properties can be improved upon by alloying and heat treatment of ductile iron to obtain targeted matrix structure(s) that can serve as high wear resistance material [3]. Heat treatment of ductile irons to improve wear resistance is majorly done by austempering the iron at different temperatures [4]. This austempering process involves different stages which must be carefully carried out to achieve the desired result. Also the costs involved are quite enormous, compared to alloying with little quantity of alloying materials. Other methods of improving wear resistance of ductile irons are now in practice, and some result in non-homogeneous properties in the ductile irons. For instance, Qi et al [5] achieved high surface hardness and improved wear resistance by

depositing WC- 12 % Co on ductile iron by electric contact surface strengthening. Improved results were obtained in all the coated samples than the ductile iron substrate that was not coated. However, the nodules at the coated surfaces seemed distorted – an occurrence which could impair the properties of ductility, strength and other properties conferred on the iron as a result of the presence of 'good' nodules. Ceccarelli et al. [6], partially chilled ductile iron in other to achieve high abrasion and impact properties, by using chills at selected location in the mould to increase the rate of solidification at that region so as to obtain carbide at the location. Low wear rate in samples with carbide and pearlitic matrix was achieved but very low impact toughness because of the high carbide content. In other words, it would have been better to work towards producing pearlitic matrix phase without carbide which causes brittleness, and still maintain appreciable impact toughness in the material. Abedi et al. [7], investigated the sliding wear behaviour of a ferritic –pearlitic ductile cast iron with different nodule count; it was discovered that abrasive wear resistance of the ductile iron decreases with increase in nodule count. This was as a result of low mechanical resistance of graphite, which implies that only possession of nodules cannot guarantee adequate wear resistance. Little studies have been reported on the behaviour of low alloyed ductile irons to abrasive and wear resistance most especially when the low alloyed ductile iron is tailored to increasing the pearlitic matrix of the ductile iron. Utilizing low alloyed ductile iron with molybdenum, nickel, chromium and copper will help in reduction in material cost. It will also give rise to carbide free components that potentially can reduce significantly the embrittlement and low impact resistance of ductile irons. There will also be possession of uniform properties across the ductile irons. The confirmation of these assertions necessitated the evaluation of the wear and fracture toughness of pearlite enriched ductile irons in this study.

2. MATERIALS AND METHODS

2.1 Materials

Materials used for the production of the pearlitic-ferritic ductile irons are; gray cast iron scrap, graphitizer, calcium carbonate as flux for slag removal and calcium carbide for desulphurizing the melt. Materials used for alloying are ferromanganese (containing 80 % Mn), ferrochrome (containing 64 % Cr), ferromolybdenum (with 72 % Mo), copper in the form of wire and ferrosilicon magnesium containing 5 % Mg and 42 % Si for inoculation and nodularization.

2.2 Production of the Irons

Melting was carried out in an oil fired lift out crucible furnace. Standard procedures were followed in accordance with Ziolkowski and Wrona [8], Khanna, [9], to prepare the charge materials melted in the furnace. This was done to enhance the quality of the melt obtained by following equation 1 to prepare the charges. Charges were then heated in a removable graphite crucible inserted in the furnace to temperature above 1300 ^{0}C, before adding calcium carbide for desulphurization of the melt in accordance with Oyetunji and Omole, [10]. The aim of desulphurizing the melts with calcium carbide is to avoid the consumption of the Mg meant for nodulization from being used up to desulphurize the melt. The melts produced were superheated to temperature of 1420 ^{o}C, tapped and treated with $FeSi_{42}Mg_5$ in a ladle built to conform to sandwich process of adding Mg into melt, [11]. This sandwich process helps to achieve high magnesium recovery and prevent 'fading' of the ferroalloy. The melts were cast in green sand mould to obtain cylindrical rod ø20 mm X 200 mm length. The chemical composition of the ductile irons produced was determined using Tasman absorption spectrometer with argon gas accessory for sparking the specimens' surfaces. Composition result of the ductile irons is shown in Table 1.

$$\text{Material needed} = \frac{(\text{Expected amount} - \text{Amount in base metal})\ \text{Charge capacity}}{Yield\ (purity)\ of\ the\ alloying\ material} \quad (1)$$

2.3 Microstructures Characterization

Zeiss optical microscope with Axiocam5 camera attachment was used for structural characterization of the castings produced. Specimens were prepared through the process of grinding and polishing using different grits and pastes. Mirror polished specimens were etched in

4 % nital , swabbing in water for 10 to 15 seconds after which the microstructures were examined with the Zeiss microscope. The phases present in the microstructures were quantitatively analyzed using ImageJ software application.

2.4 Hardness Test

Hardness of the ductile irons produced was performed on each specimen by grinding the surface and using INNOVATEST FALCON 500 micro hardness testing machine in accordance with ASTM E29 – 16 standard. [12]. Test load of 0.1 Kg was applied on each specimen with dwell time of 10 seconds. Five different locations were selected for measurement and average of the five readings was used as the hardness result.

2.5 Fracture Toughness

Circumferential notch tensile specimens (CNT) were used to determine the fracture toughness of the materials in accordance with Alaneme, [13]. The specimens for the test were machined to gauge length of 40 mm, gauge diameter (D) of 6 mm, notch diameter (d) of 4.2 mm and notch angle of 60 ^{0}. An Instron universal testing machine, operated at a quasi-static strain rate of 10^{-3} mm/s was used to subject the specimens to tensile loading to fracture at room temperature. The load to fracture (P_f) of each specimen was obtained from the CNT specimens load-extension plot. The tensile load – extension plots obtained are presented in Fig. 1. This was used to evaluate the fracture toughness using the relation in (2) according to Dieter, [14]:

$$K_{IC} = \frac{Pf}{D^{3/2}} \left[1.72\left(\frac{D}{d}\right) - 1.27\right] \quad (2)$$

Where D and d are the gauge diameter and notched section diameter respectively. Using the relations in (3) in accordance with Nath and Das, [15], validity of the fracture toughness values obtained was determined.

$$D \geq \left(\frac{Kic}{\sigma y}\right)^2 \quad (3)$$

Table 1. Chemical Composition of Ductile irons.

Melt	CE	% C	% Si	% Mn	% Mo	% Ni	% Cr	% Cu	% Mg	% S	% P
D_1	4.27	3.42	2.50	0.352	0.103	0.165	-	0.20	0.073	0.03	0.048
D_2	4.38	3.50	2.60	0.39	0.19	0.22	-	-	0.086	0.034	0.042
D_3	4.14	3.20	2.80	0.53	-	-	0.12	0.21	0.095	0.026	0.030
D_4	4.23	3.40	2.45	0.50	0.24	0.181	0.102	-	0.09	0.031	0.048
D_5	4.18	3.30	2.62	0.42	-	-	-	-	0.081	0.027	0.029

Where:

$Carbon\ Equivalent\ (CE) = TC\% + \frac{Si\ \%+P\ \%}{3}$ (4) and the percentages are in wt.%

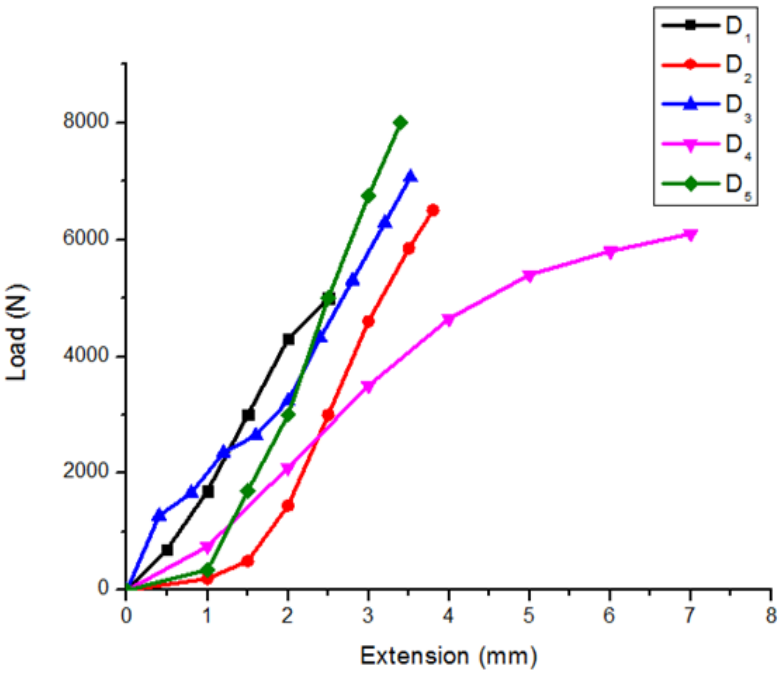

Fig. 1. Plot of Load-Extension Circumferential Notch Specimens for Fracture Toughness Test.

2.6 Wear Test

Wear test was carried out on Anton Paar Tribometer (TRB) machine, based on pin-on-disk with stainless steel indenting ball of radius 5 mm. This was done in accordance with ASTM G99- 05 -16 standard [16].

Contact load of 10 N was applied on all the specimens at a speed of 150 revolutions per minute (rpm) and linear speed of 7.85 cm/s for 30 minutes. For the total time of 30 minutes utilized for the test, sliding distance of 141 m was covered. Volumetric wear rate was estimated in accordance with Agbeleye et al. [17] by measuring the weight loss in each sample after each test. The weight loss for each sample material was calculated from the difference in weight before and after the experiment, and was used to calculate the wear volume and specific wear rate as follows:

$$Wear\ Volume = \frac{Wear\ Mass}{Density} \quad (5)$$

$$Specific\ Wear\ Rate = \frac{Wear\ Volume}{Sliding\ Distance\ X\ Force\ Applied} \quad (6)$$

The specific weight value used for the computation is 7.87 g/cm^3.

The worn samples were taken for measurement and analyzed using scanning electron microscope.

3. RESULTS AND DISCUSSION

3.1 Microstructures

The microstructures of the ductile irons produced are presented in Figure 2. The microstructures show the presence of nodules in all the samples. This is an indication that the production process adopted yielded ductile irons. The quantitative analysis of the microstructures is presented in Table 2. The Table shows that the microstructures of each composition contain considerable nodules count, indicative of good nodules formation. The volume of pearlite content increased in the micro alloyed samples in the range of 62.25 % minimum to 93.86 % maximum as compared to the unalloyed sample (D_5). This increase was due to the interaction of the alloying elements (Mo, Ni, Cr and Cu) which help in forming tiny pearlite distributed within the structures. The increase in pearlite content, relatively lower ferrite, and the morphology of the nodules in the microstructures of the produced micro alloyed ductile irons; account for the increase in mechanical properties of the ductile irons.

Table 2. Microstructural Analysis of the Ductile Irons.

Sample	Volume fraction of Pearlite	Volume fraction of Ferrite	Volume fraction of Nodule	Nodularity %	Nodules count (per mm^2)
D_1	49.38 % ±2.55	38.93 % ±2.35	11.14 % ±1.82	91	110
D_2	49.70 % ±2.82	40.11 % ±2.64	10.98 %±1.68	90	115
D_3	56.06% ±1.85	29.83 % ±2.43	14.51 %±2.08	88	105
D_4	56.59 % ±2.32	32.68 % ±2.42	11.31 %±1.95	92	120
D_5	30.63 % ±2.12	59.37 % ±2.71	10.27 % ±2.10	88	107

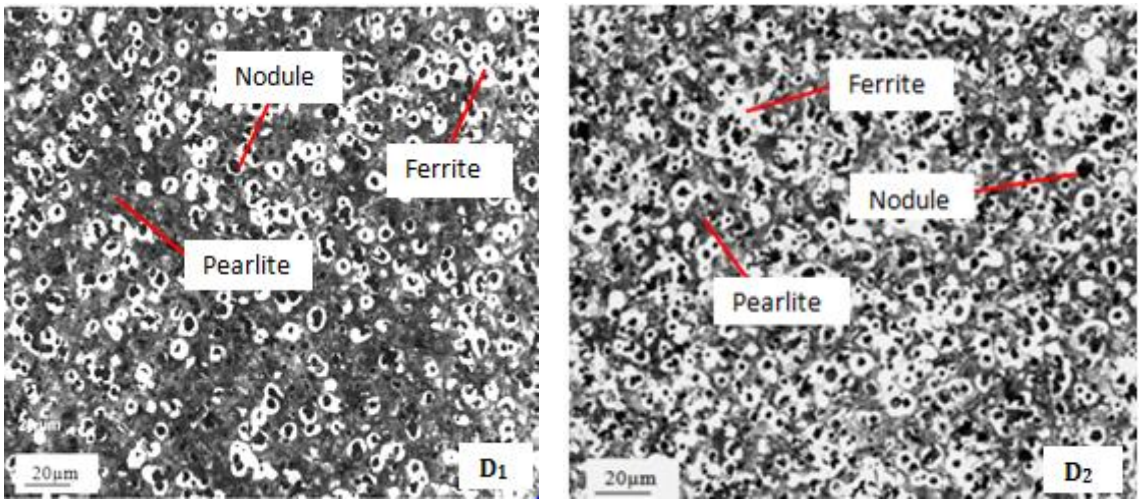

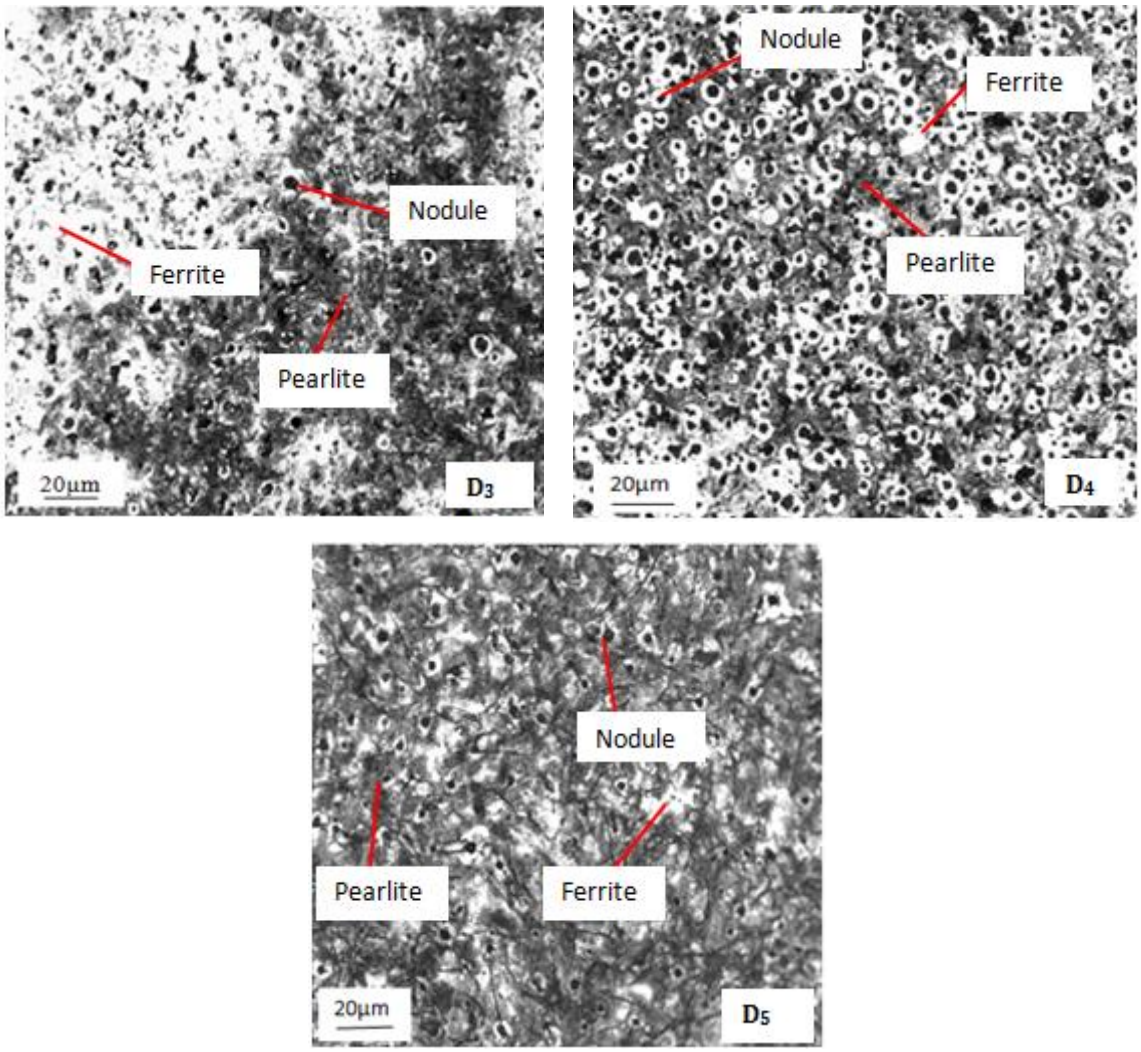

Fig. 2. Optical Micrographs of the Ductile Irons.

3.2 Hardness Result

Variation of hardness of the ductile irons produced is shown in Fig. 3. It is observed that samples D_1 to D_4 have hardness values higher than the ductile iron without any alloying addition (D_5). The range of increase in hardness values compared to unalloyed sample varies from 1.41 % to 36.47 % using the % ratio. Specifically, the composition D_4 (containing Mo, Ni, and Cr) had the highest hardness value, followed by D_3 (which contains Cr and Cu), D_1 (Mo, Ni and Cu), D_2 (Mo and Ni) and then D_5 (control composition) in decreasing order. This increase is attributable to the increase in pearlite in the microstructure of the alloyed samples which is in the range 62.25 % to 93.86 % (compared with the pearlite content of the control ductile iron composition D_5). The pearlite phase increases the hardness and mechanical properties of the ductile irons since it contains a relatively hard phase, which contributes to matrix strengthening [18].

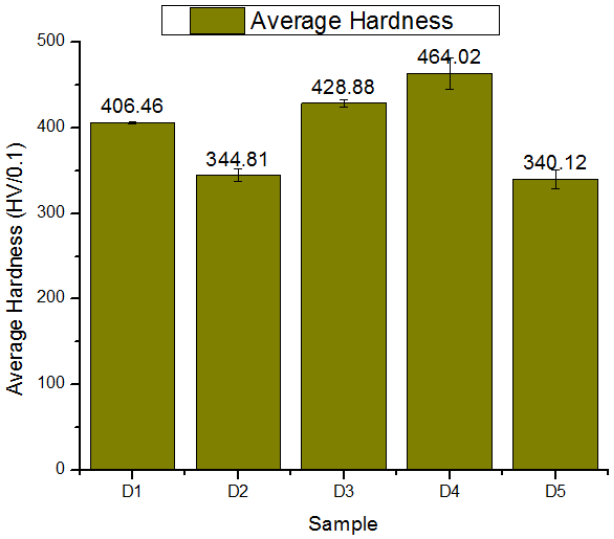

Fig. 3. Variation of Hardness of the Ductile Iron.

3.3 Fracture Behaviour

Fracture toughness values of the ductile irons produced are presented in Fig. 4. Samples D_3 and D_4 have the highest fracture toughness with 5.5 % and 25.2 % increase respectively compared to the unalloyed sample (sample D_5). This is an indication that Cu and Cr in sample D_3 as well as Mo, Ni and Cr addition in sample D_4 have increased the toughness of the ductile iron than that of sample D_5 that did not contain any addition. The two compositions also contained the highest proportion of pearlite (56.06 % and 56.59 %); and also possessed higher capability to resist crack propagation than the other compositions produced. The improved fracture toughness with increased pearlite content was not consistent as the compositions designated D_1 and D_2, showed lower values than sample D_5 (composition without micro alloying addition) despite containing relatively higher pearlite contents.

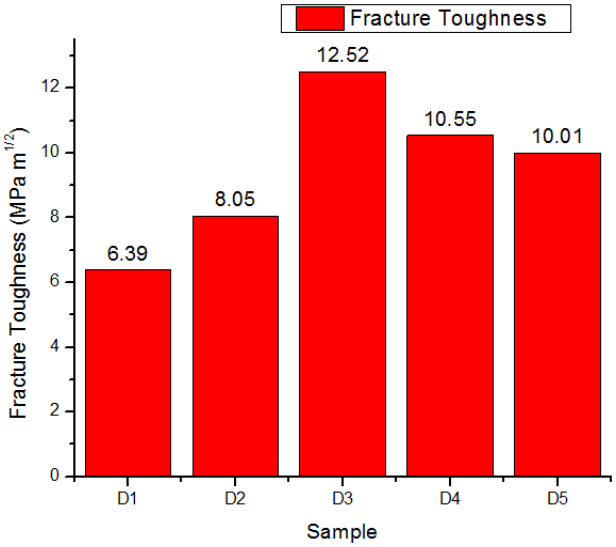

Fig. 4. Fracture Toughness of the Ductile Irons.

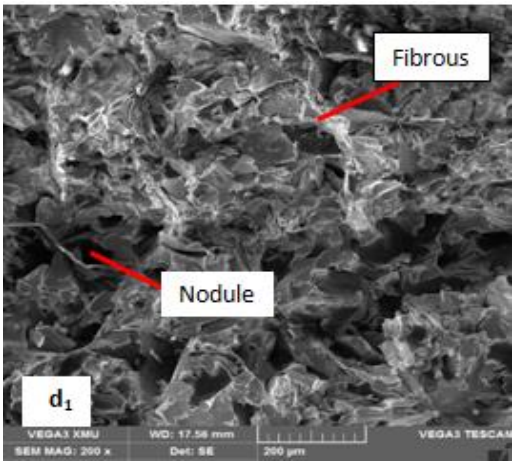

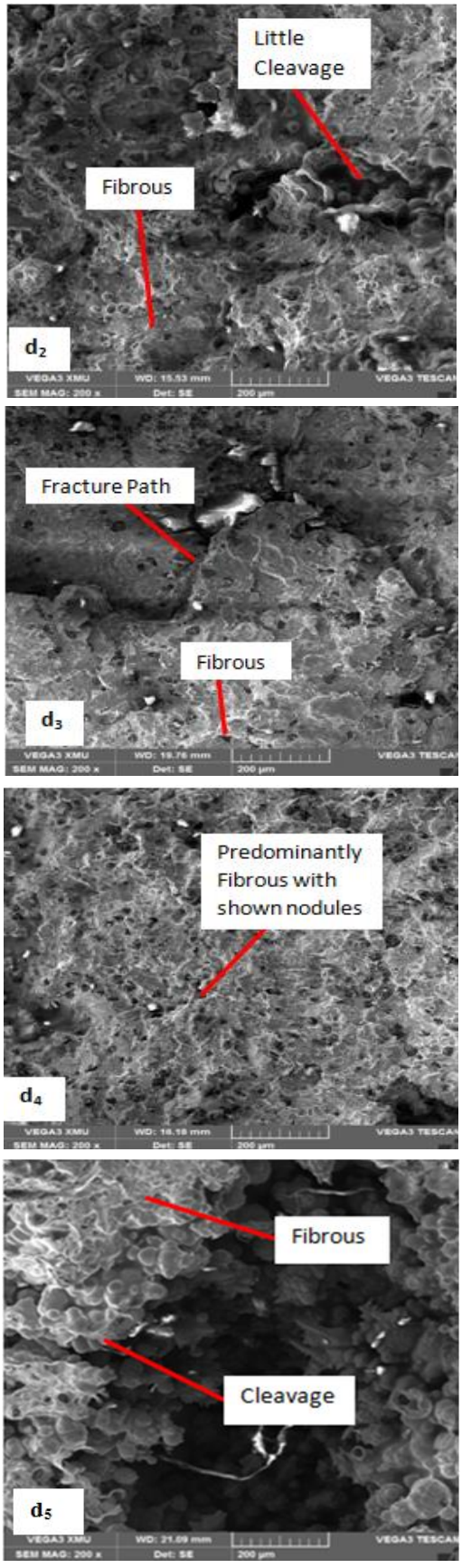

Fig. 5. Fracture Morphology of the Ductile Irons (with denotations d_1, d_2, d_3, d_4 and d_5 represent sample D_1, D_2, D_3, D_4 and D_5 respectively).

The fracture morphology of the material is shown in Fig. 5. The revealed structures of the fracture surfaces showed fibrous fracture with some traces of cleavage in samples D_1, D_2 and D_5. Sample D_4 that contains fibrous structure is with nodules seen on its fracture surface. This is an indication of mixed mode fracture and may be due to pearlitic-ferritic type of matrix possessed by the ductile irons. Pearlite as a hard phase can induce the cleavage structure, while the ferrites and the presence of nodules will give ductility to the iron, hence fibrous structure [19,20].

3.4 Wear Rate

Variation of specific wear rates of the ductile irons is presented in Fig. 6. Alloyed samples exhibit lower wear rate in comparison to the unalloyed sample.

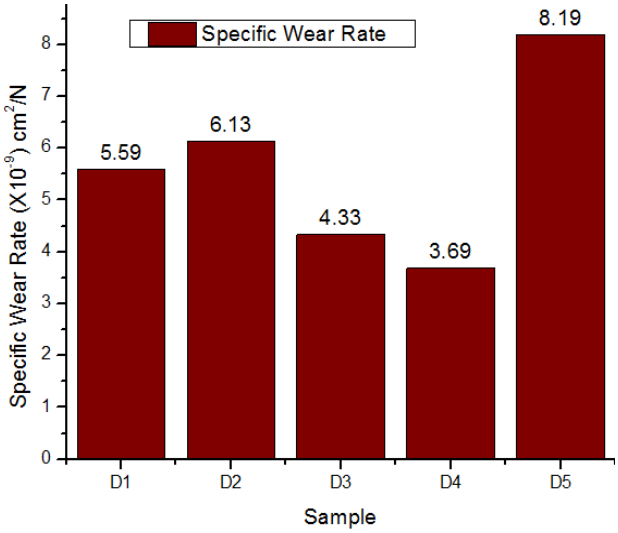

Fig. 6. Specific Wear Rate of the Ductile Irons Produced.

The percentage of increase in wear rate of unalloyed sample to the alloyed samples D_1, D_2, D_3 and D_4 are 46.7 %, 33.7 %, 89.5 % and 121.9 % respectively. Sample D4, therefore presented the most superior wear resistance of all the samples. Generally, the wear rates obtained reduce with increase in hardness of the ductile iron, which is in accordance with Zhang et al. [21] and Murthy et al. [22]. Increase in hardness values of the alloyed samples than the unalloyed one was achieved as a result of the increase in pearlite contents and reduction in the ferrite contents present in the micro alloyed samples in comparison to the unalloyed sample D_5. This increase in hardness contributed to the lower specific wear rate. The worn surface of the samples shows plastic shear deformation; which is due to the frictional force at the surface of the specimens against the pin when test was conducted. This is also in accordance with Zhang et al. [23]. Therefore the wear mechanism is considered as delamination.

There is an increase in the coefficient of friction of the alloyed samples in comparison with the unalloyed sample D_5. The increase, relative to that of sample D_5, ranged between 3.64 to 60.11 %, with sample D_4 having the highest value. It is also observed that coefficient of friction of the ductile irons increases correspondingly with the increase in their hardness. The wear tracks micrographs of the ductile irons are presented in Fig. 7. Also the coefficient of friction of the various samples is shown in Fig. 8.

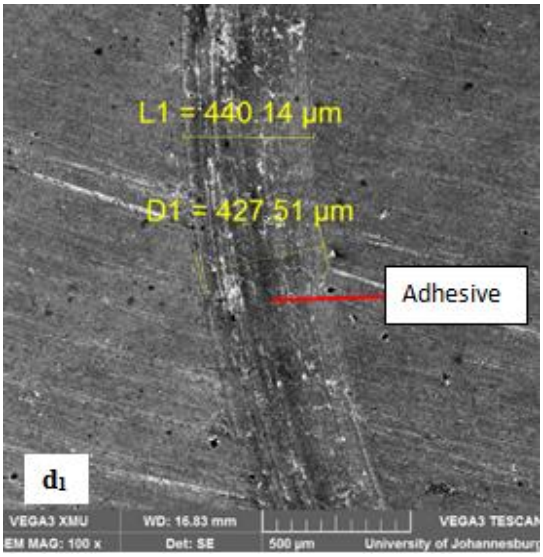

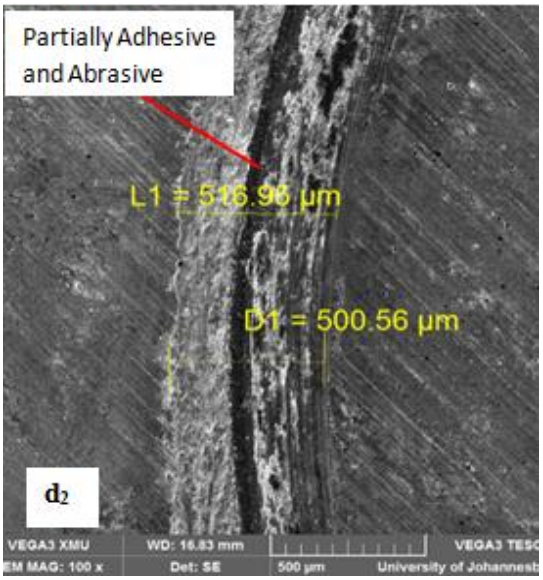

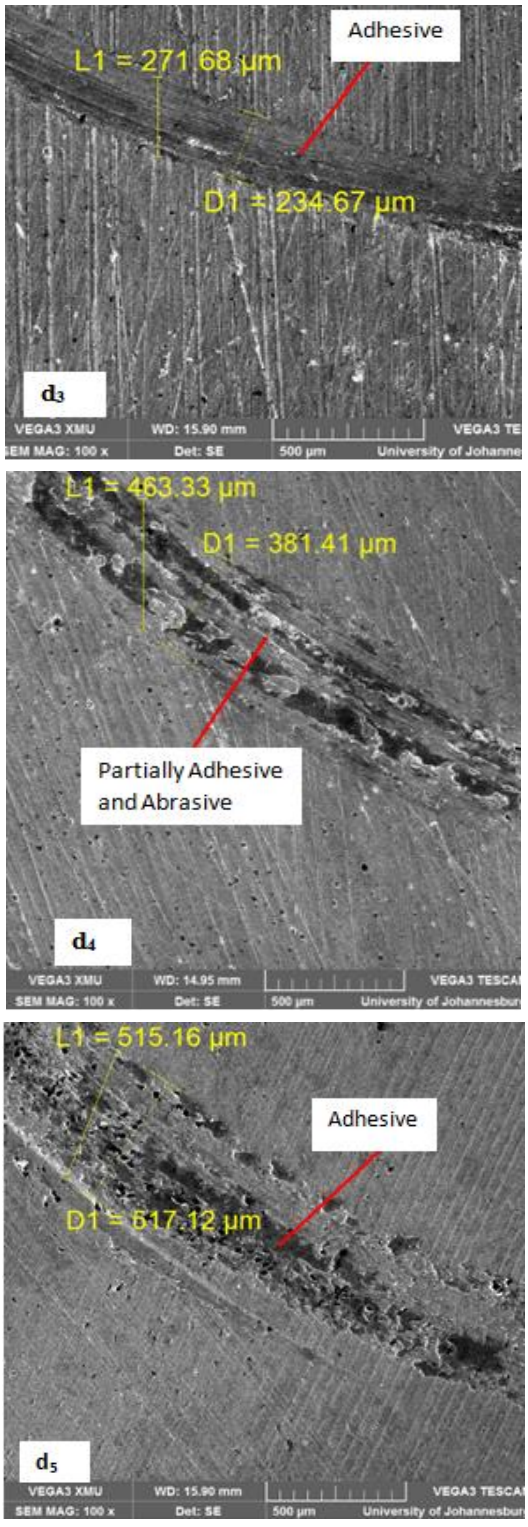

Fig. 7. Wear Tracks Obtained with SEM (samples D_1, D_2, D_3, D_4 and D_5 are denoted by d_1, d_2, d_3, d_4 and d_5 respectively).

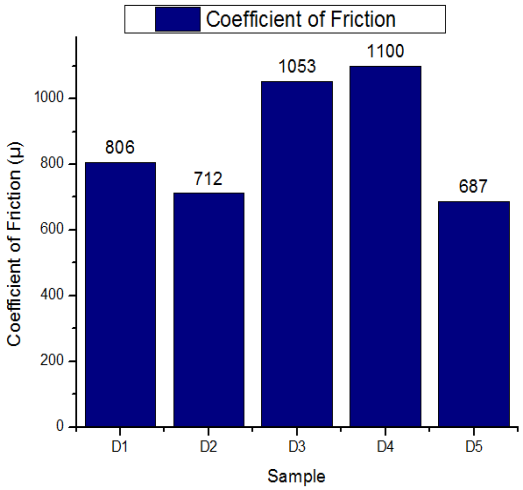

Fig. 8. Coefficient of Friction of the Ductile Irons.

The wear tracks are seen to contain primarily adhesive wear debris, with the exceptions of samples D_2 and D_4, which contained mixtures of adhesive and abrasive wear patterns. The wear surface morphology hence suggests that adhesive wear as the dominant wear mechanism in most of the ductile irons produced. Bedolla-Jacuinde et al. [24] reported that wear particles from ferrous materials consist of iron oxides that are mixtures of FeO and Fe_2O_3. The iron oxide particles are harder than pearlite, therefore the adhered particles will provide relatively hard coating on the surface and reduce the wear rate of the ductile irons.

Table 3 summarizes the dependence of the evaluated properties on the microstructure (pearlite and nodule proportion) of the ductile irons. It is observed that samples D_3 and D_4 which have the highest pearlite contents, also have the highest hardness values, fracture toughness and lowest wear rates. Other ductile iron compositions containing alloying additions (D_1 and D_2) which also have higher pearlite content than the control sample (D_5), possess higher hardness and lower wear rate than the control sample. However, the fracture toughness values of D_1 and D_2 were lower than that of the control sample. This suggests that the hardness and wear rates of the ductile irons showed more dependence on pearlite content compared to the fracture toughness.

Table 3. Dependence of Evaluated Properties on Microstructure (pearlite content and nodules count).

Sample	Pearlite Content (%)	Nodules count Per mm²	Hardness HV/0.1	Fracture Toughness MPa √m	Wear rate X10⁻⁹ Cm²/N
D_1	49.38	110	406.46	6.39	5.59
D_2	49.70	115	344.81	8.05	6.13
D_3	56.06	105	428.88	12.52	4.33
D_4	56.59	120	464.02	10.55	3.69
D_5	30.63	107	340.12	10.01	8.19

4. CONCLUSION

The fracture characteristics and wear behaviour of ductile irons micro-alloyed with combinations of Cr, Cu, Mo, and Ni to achieve a pearlite enriched matrix was investigated in this study.

The results obtained show that:

1. There is combination of fibrous and cleavage structure seen on the fracture surfaces, which shows that there is ductile as well as brittle transition failure in the material, but the ductile transition, is more dominant. That occurrence may be due to the matrix (pearlitic-ferritic) possessed by the ductile irons.
2. The specific wear rate of the samples decreases with increase in hardness of the material. Values of coefficient of friction obtained also increases as hardness increases.
3. Both adhesive and abrasive wear was noticed to have taken place. Majorly the adhesive wear was more, which is perceived to help in the reduction of the specific wear rate of the material.
4. Samples D_4 and D_3 with highest fracture toughness have lowest specific wear rate, while sample D_5 with relatively higher fracture toughness compared to samples D_1 and D_2 have higher specific wear rate than samples D_1 and D_2.

Acknowledgement

The authors show appreciation to the Head and Members of Advanced Materials and Electrochemical Technology Research Group, University of Johannesburg, South Africa, for their assistance and use of facilities for this research work.

REFERENCES

[1] Y. Sahin, O. Durak, *Abrasive Wear Behavoiur of Austempered Ductile Iron,* Materials & Design vol. 28, iss. 6, pp. 1844–1850, 2007, doi: 10.1016/j.matdes.2006.04.015

[2] X. Meng, C. Fang, K. Niu, *Tribological Behavior Anisotropy in Sliding Interaction of Asperities on Single-Crystal α-Iron: A Quasi-Continuum Study*, Tribology International, vol. 118, pp. 347-359, 2018, doi: 10.1016/j.triboint.2017.10.012

[3] O. Gutnichenko, V. Bushlya, J. Zhou, J.-E. Stahl, *Tool Wear and Machining Dynamics when Turning High Chromium White Cast Iron with pcBN Tools,* Wear, vol. 390–391, pp. 253-269, 2017, doi: 10.1016/j.wear.2017.08.005

[4] A. Zammit, S. Abela, L. Wagner, M. Mhaede, M. Grech, *Tribological Behaviour of Shot Peened Cu–Ni Austempered Ductile Iron*, Wear, vol. 302, iss. 1-2, pp. 829-836, 2013, doi: 10.1016/j.wear.2012.12.027

[5] X. Qi, S. Zhu, H. Ding, Z. Zhu, Z. Han, *Microstructure and Wear Behaviors of WC 12%Co Coating Deposited on Ductile Iron by Electric Contact Surface Strengthening,* Applied Surface Science, vol. 282, pp. 672–679, 2013, doi: 10.1016/j.apsusc.2013.06.032

[6] B.A. Ceccarelli, R.C. Dommarco, R.A. Mart´ınez, M.R. Mart´ınez Gamba, *Abrasion and Impact Properties of Partially Chilled Ductile Iron,* Wear, vol. 256, iss. 1-2, pp. 49–55, 2004, doi: 10.1016/S0043-1648(03)00257-6

[7] H.R. Abedi, A. Fareghi, H. Saghafian, S.H. Kheirandish, *Sliding Wear Behavior of a Ferritic–Pearlitic Ductile Cast Iron with Different Nodule Count,* Wear, vol. 268, iss. 3-4, pp. 622-628, 2010, doi: 10.1016/j.wear.2009.10.010

[8] E. Ziolkowski, R. Wrona, *Using Fuzzy Optimization Method in Calculation of Charge Burden to Correct the Chemical Composition of Metal Melt,* Archives of Foundry Engineering, vol. 7, iss. 3, pp. 183-186, 2007.

[9] O.P. Khanna, *Materials Science and Metallurgy*, New Delhi: Dhanpat Rail Publication, 2009.

[10] A. Oyetunji, S.O. Omole, *Achievement of Nodules in Ductile iron Having Sulphur Content not less than 0.07 % Weight,* Daffodil International University Journal of Science and Technology, vol. 9, iss. 2, pp. 43-47, 2014.

[11] M. Ramadan, N. Fathy, *Influence of Semi-Solid Isothermal Heat Treatment on Microstructure and Mechanical Properties of Ductile Cast Iron,* Journal of Minerals and Materials Characterization and Engineering, vol. 2, no. 1, pp. 26-31, 2014, doi: 10.4236/jmmce.2014.21005

[12] ASTM E29, *Standard Test Methods for Micro Hardness of Metallic Materials,* ASTM International, West Conshohocken, PA, 2016.

[13] K.K. Alaneme, *Fracture Toughness (Kic) Evaluation for Dual Phase Low Alloy Steels Using Circumferential Notched Tensile (CNT) Specimens,* Materials Research, vol. 14, no. 2, pp. 2011, doi: 10.1590/S1516-14392011005000028

[14] G.E. Dieter, Mechanical Metallurgy, Singapore: McGraw-Hill, 1992.

[15] S.K. Nath, U.K. Das, *Effect of Microstructure and Notches on the Fracture Toughness of Medium Carbon Steel,* Journal of Naval Architecture and Marine Engineering, vol. 3, pp. 15–22, 2006.

[16] ASTM G99 – 05, *Standard Test Method for Wear Testing with a Pin-on-disk Apparatus* ASTM, International, West Conshohocken, PA, 2016.

[17] A.A. Agbeleye, D.E. Esezobor, S.A. Balogun, J.O. Agunsoye, J. Solis, A. Neville, *Tribological Properties of Aluminium-Clay Composites for Brake Disc Rotor Applications,* Journal of King Saud University – Science, in press, doi: 10/1016/j.jksus.2017.09.002

[18] R.A. Gonzaga, P.M. Landa, A. Perez, P. Villanueva, *Mechanical Properties Dependencyof the Pearlite Content of Ductile Iron*, Journal of Achievements in Materials and Manufacturing Engineering, vol. 33, iss. 2, pp. 150-158, 2009.

[19] F. Alabassian, S.M.A. Boutorabi, S. Kheirandish, *Effect of Inoculation and Casting Modulus on the Microstructure and Mechanical* P*roperties of Ductile Ni-Resist Cast ron*, Material Science and Engineering: A, vol. 651, pp. 467-473, 2016, doi: 10.1016/j.msea.2015.09.024

[20] J. Serrallach, J. Lacaze, J. Sertucha, R. Suárez, A. Monzón, *Effect of Selected Alloying Elements on Mechanical Properties of Pearlitic Nodular Cast Irons,* Key Engineering Materials, vol. 457, pp. 361–366, 2011, doi: doi: 10.4028/www.scientific.net/KEM.457.361

[21] N. Zhang, J. Zhang, L. Lu, M. Zhang, D. Zeng, Q. Song, *Wear and Friction Behavior of Austempered* D*uctile Iron as Railway Wheel Material*, Materials & Design, vol. 89, pp. 815–822, 2016, doi: 10.1016/j.matdes.2015.10.037

[22] K.N. Murthy, P. Sampathkumaran, S. Seetharamu, *Abrasion and Erosion Behaviour of Manganese Alloyed Permanent Moulded Austempered Ductile Iron,* Wear, vol. 267, iss. 9-10, pp. 1393–1398, 2009, doi: 10.1016/j.wear.2008.12.033

[23] J. Zhang, N. Zhang, M. Zhang, D. Zeng, Q. Song, L. Lu, *Rolling–Sliding Wear of Austempered Ductile Iron with Different Strength Grades*, Wear, vol. 318, iss. 1-2, pp. 62–67, 2014, doi: 10.1016/j.wear.2014.06.015

[24] A. Bedolla-Jacuinde, F.V. Guerra, M. Rainforth, I. Mejia, C. Maldonado, *Sliding Wear Behaviour of Austempered Ductile Iron Micro Alloyed with Boron,* Wear, vols. 330-331, pp. 23- 31, 2015, doi: 10.1016/j.wear.2015.01.004